

Supplemental Material

Perforin-deficient CAR-T cells recapitulate late-onset inflammatory toxicities observed in patients

Kazusa Ishii^{1,2,3}, Marie Pouzolles^{1†}, Christopher D. Chien^{1†}, Rebecca A. Erwin-Cohen⁴, M. Eric Kohler^{1,5}, Haiying Qin¹, Haiyan Lei¹, Skyler Kuhn^{6,7}, Amanda K. Ombrello⁸, Alina Dulau-Florea⁹, Michael A. Eckhaus¹⁰, Haneen Shalabi¹, Bonnie Yates¹, Daniel A. Lichtenstein¹, Valérie S. Zimmermann^{1,11}, Taisuke Kondo¹, Jack F. Shern¹, Howard A. Young^{4,12}, Naomi Taylor^{1,11}, Nirali N. Shah^{1*} and Terry J. Fry^{1,5*}

¹Pediatric Oncology Branch, Center for Cancer Research (CCR), National Cancer Institute (NCI), National Institutes of Health (NIH), Bethesda, MD 20892; USA

²Hematology Branch, National Heart, Lung, and Blood Institute, NIH, Bethesda, MD, 20892; USA

³Experimental Transplantation and Immunotherapy Branch, CCR, NCI, NIH, Bethesda, MD 20892; USA

⁴Cancer and Inflammation Program, CCR, NCI, NIH, Frederick, MD, 21702; USA

⁵Department of Pediatrics, University of Colorado Anschutz Medical Campus and Children's Hospital Colorado, Aurora, CO, 80045; USA

⁶CCR Collaborative Bioinformatics Resource (CCBR), CCR, NCI, NIH, Bethesda, MD 20892; USA

⁷Advanced Biomedical Computational Science, Frederick National Laboratory for Cancer Research, Frederick, MD, 21702; USA

⁸Inflammatory Disease Section, National Human Genome Research Institute, NIH, Bethesda, MD, 20892; USA

⁹Department of Laboratory Medicine, NIH, Bethesda, MD 20892; USA

¹⁰Diagnostic and Research Services Branch, Division of Veterinary Resources, NIH, Bethesda, MD 20892; USA

¹¹Université de Montpellier, IGMM, CNRS, Montpellier, France

¹²Laboratory of Cancer Immunometabolism, CCR, NCI, NIH, Frederick, MD 21702; USA

*Co-Senior Authors. †Co-Second Authors

This PDF file includes:

Figure S1. Low in vitro proliferation of Prf^{-/-} CAR-T is not rescued by IFN γ neutralization

Figure S2. Manufacturing of CD8⁺ and CD4⁺ purified CAR-T cells

Figure S3. Activated Prf^{-/-} CAR-T exhibit an inflammatory gene expression profile

Figure S4. Lack of perforin affects cytotoxicity of both CD8⁺ and CD4⁺ CAR-T cells

Figure S5. In vivo kinetics and phenotypes of CD4⁺ CAR-T cells

Figure S6. Phenotype of recipient-derived CD4⁺ T cells

Figure S7. IL-33 transcripts and kinetics of serum cytokine levels in CAR-T recipients

Figure S8. Gating strategy used for flow cytometry analyses of WT and Prf^{-/-} CAR-T following co-infusion into leukemia-bearing mice

Figure S9. The effects of IFN γ neutralization on anti-leukemia cytotoxicity and phenotypes of CAR-T

Table S1. Antibodies and reagents used for flow cytometry analysis

Table S2. Sequences of primers used for qPCR

Table S3. List of differentially expressed genes (greater than 2-fold changes) comparing Prf^{-/-} CD8⁺ CAR-T cells to WT CD8⁺ CAR-T cells after CAR-mediated in vitro activation

Text S1. Supplemental Methods

Text S2. Modified definition of HLH/MAS-like toxicities used in our anti-CD22 CAR-T clinical trial

Text S3. Primary HLH testing performed in anti-CD22 CAR-T trial

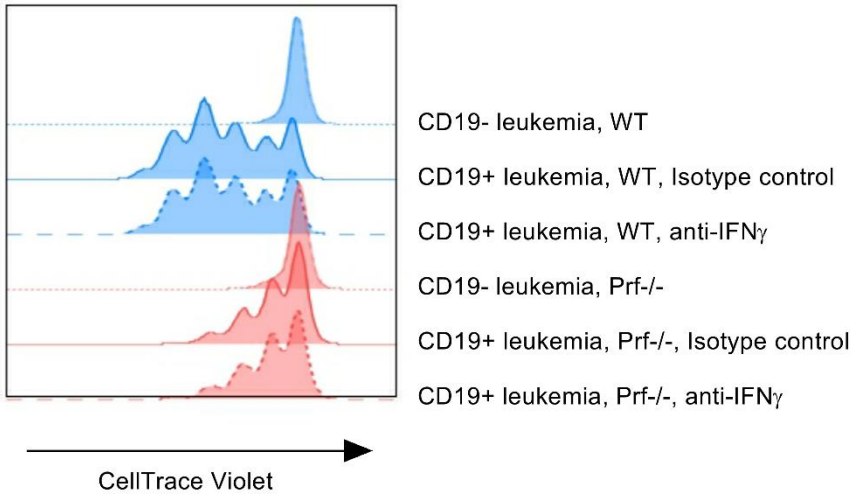


Figure S1. Low in vitro proliferation of Prf $^{-/-}$ CAR-T is not rescued by IFN γ neutralization. WT CAR-T and Prf $^{-/-}$ CAR-T were labeled with CellTrace Violet and co-cultured with GFP $^{+}$ CD19 $^{+}$ or CD19 $^{-}$ E2aPBX at an E:T ratio of 1:1 in the presence of an isotype control (rat IgG1 anti-horseradish peroxidase) or an IFN γ neutralizing antibody (clone XMG1.2) at 10 μ g/mL for 3 days. Proliferation of T cells was assessed as a function of CellTrace Violet dilution by flow cytometry. Data are representative of three replicate experiments.

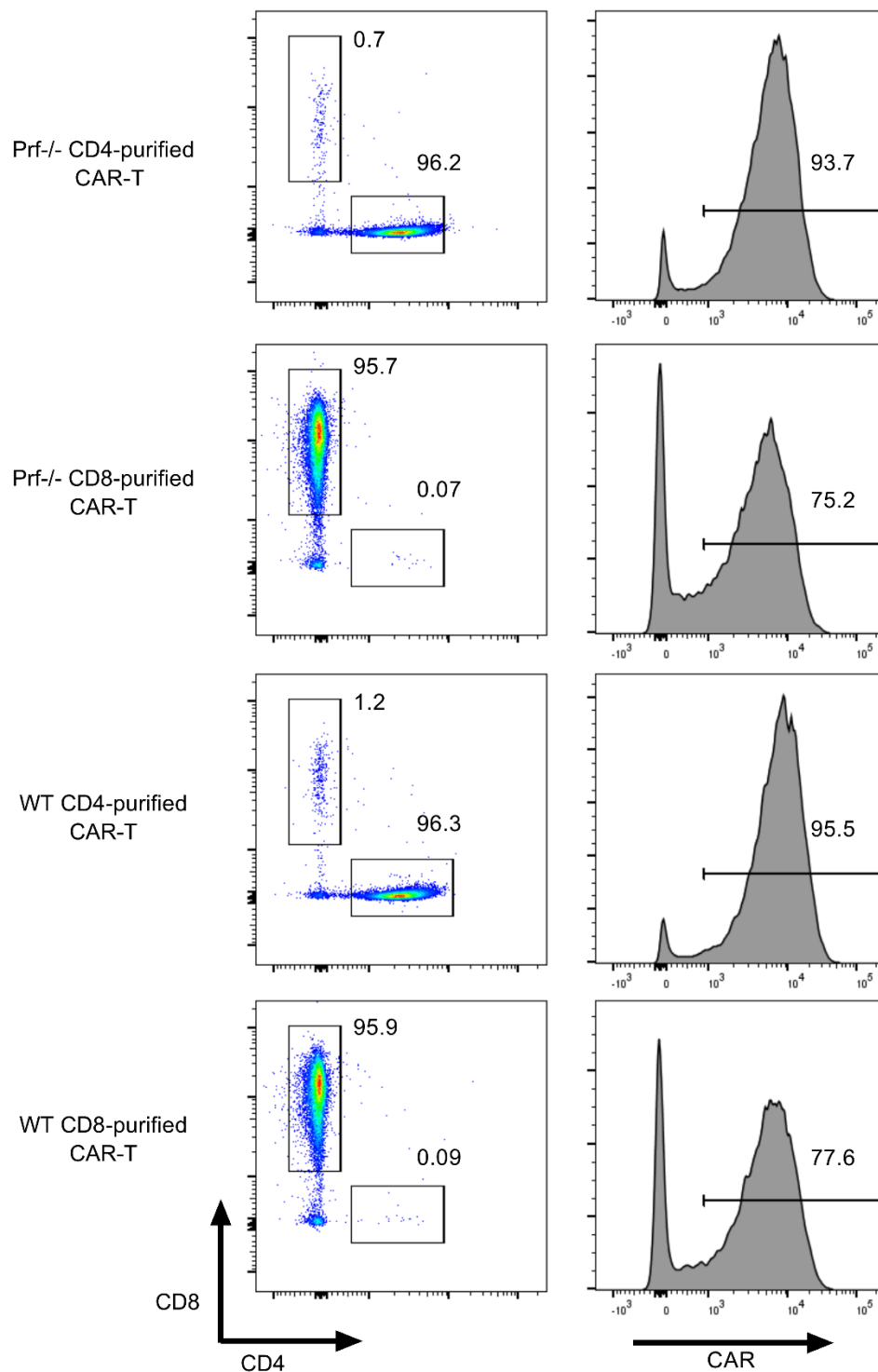


Figure S2. Manufacturing of CD8+ and CD4+ purified CAR-T cells. CD4+ and CD8+ enriched mouse splenocytes were transduced with the anti-CD19 CAR. The purity of the CD4+ and CD8+ populations (left) and transduction efficiencies (right) were evaluated by flow cytometry. Representative dot plots and histograms are shown.

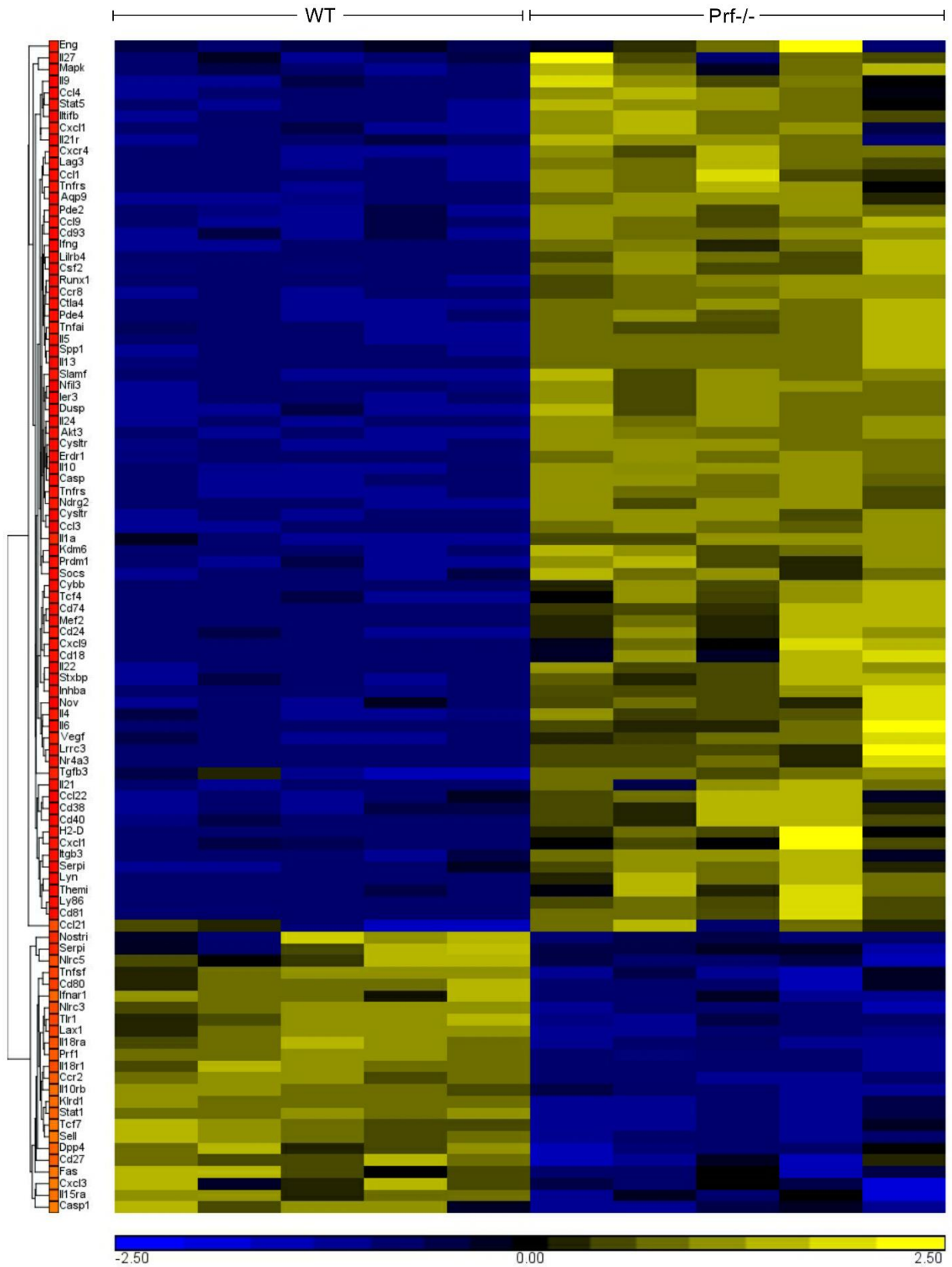


Figure S3. Activated Prf^{-/-} CAR-T exhibit an inflammatory gene expression profile. Heatmap of z-score values of 100 genes involved in inflammatory responses with more than 1.6-fold gene expression differences,

comparing CD8+ enriched Prf^{-/-} CAR-T to WT CAR-T after CAR-mediated activation. Gene expression profiling was performed as detailed in the methods (post-activation, n = 6).

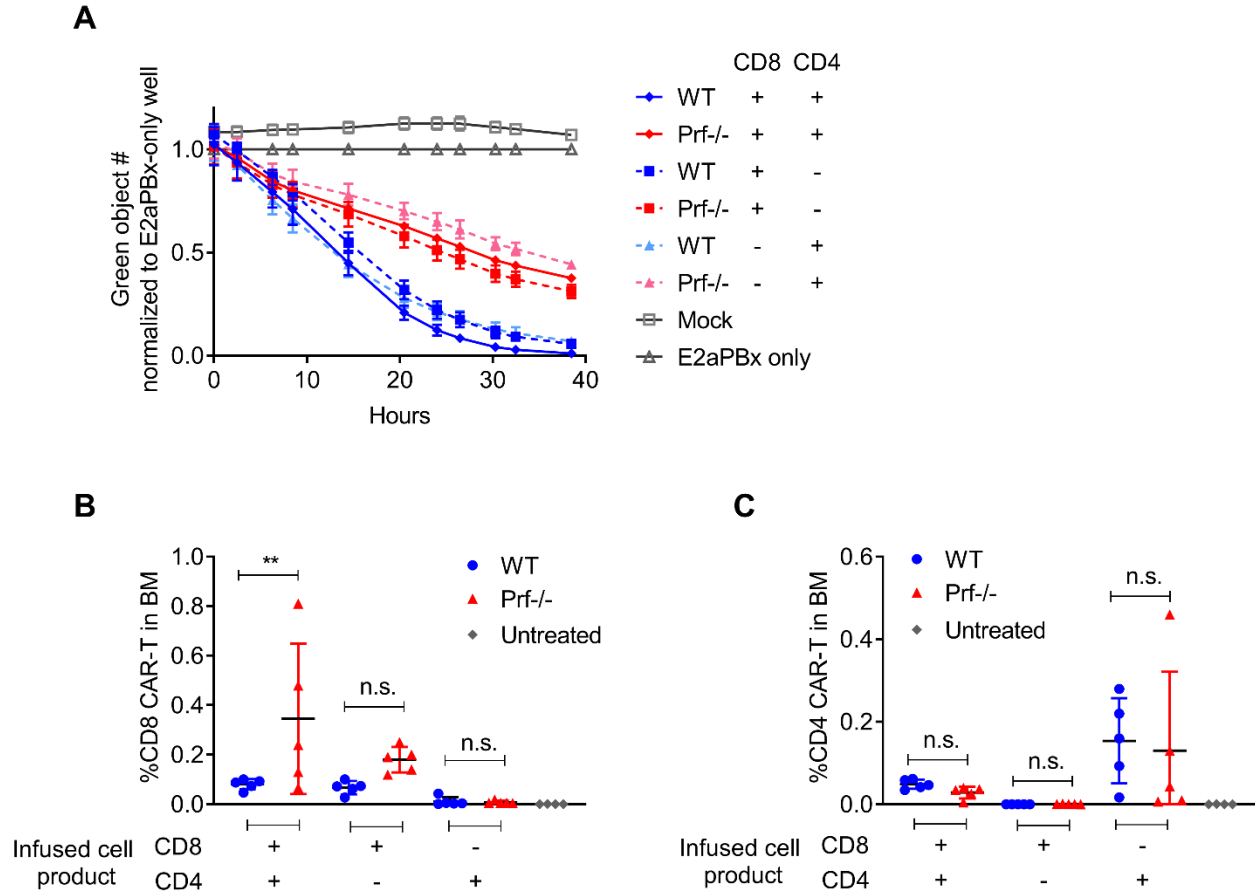


Figure S4. Lack of perforin affects cytotoxicity of both CD8+ and CD4+ CAR-T cells. CAR-T cells were manufactured from CD4+ or CD8+ purified splenic T lymphocytes. (A) In vitro cytotoxicity measured by Incucyte assay (Incucyte Zoom, Essen BioScience). GFP+ E2aPBX (3E5 cells) were co-cultured with either CD4+, CD8+, or a 1:1 mixture of CD4+ and CD8+ CAR-T (6E5 cells) at an E:T ratio of 2:1. Phase contrast and fluorescent (green) imaging were taken at indicated timepoints. GFP positive cells (green objects) were normalized to untreated control wells. (B-C) Leukemia-bearing mice were treated with either CD4+, CD8+, or a 1:1 mixture of CD4+ and CD8+ CAR-T manufactured from WT and Prf-/- donors (total CAR-T dose, 1E5 cells/mouse), according to the experimental scheme depicted in Figure 2A. (B) The percentages of CD8+ CAR-T (CD45.2+/CD8+) and (C) CD4+ CAR-T (CD45.2+/CD4+) in the bone marrow (BM) were measured by flow cytometry on day 14. Data are reported as means \pm SD (A-C). $n = 3$ (A); $n = 5$ (B, C). Figures are representative of three replicate in vitro experiments and two replicate in vivo experiments. Statistical significance was determined using one-way ANOVA with Sidak's correction (B, C). * $P < 0.05$; ** $P < 0.01$; *** $P < 0.001$; **** $P < 0.0001$; n.s. non-significant.

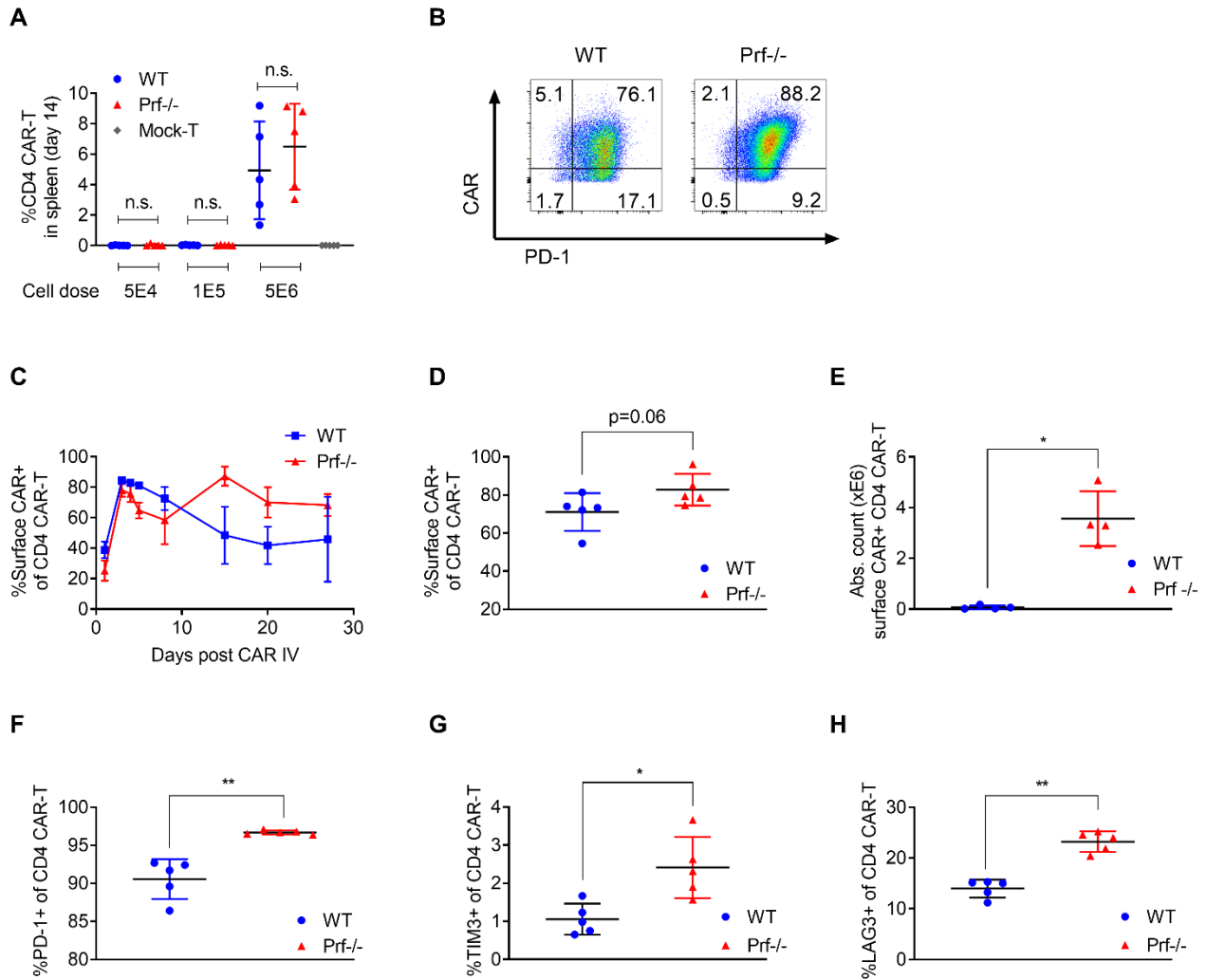


Figure S5. In vivo kinetics and phenotypes of CD4⁺ CAR-T cells. (A-D) Leukemia-bearing mice were pre-conditioned with cyclophosphamide (200 mg/kg I.P. on day -1) and injected with either 5E4, 1E5, or 5E6 WT or Prf^{-/-} CAR-T cells (CD45.2⁺) on day 0. (A) On day 14 of treatment, the percentages of CD4⁺ CAR-T (CD45.2⁺CD4⁺) within total splenocytes were evaluated. (B-E) Surface CAR-expression on CD4⁺ CAR-T in spleens of mice treated with CAR-T (5E6 cells) was evaluated with flow cytometry. (B) Representative dot plots, (C) kinetics of surface CAR⁺ cells on indicated timepoints, (D) statistical comparison of the percentages of surface CAR⁺ cells within the CD4⁺ CAR-T subset on day 14, and (E) absolute numbers of CD4⁺ CAR-T with surface CAR expression on day 14 are presented. (F-H) Expression of (F) PD-1, (G) TIM3, and (H) LAG3 were evaluated on CD4⁺ CAR-T in spleens of recipient mice 14 days after adoptive T cell transfer. Data are presented as means \pm SD (A, C-H). n = 5 (A, D, F-H); n = 4 (C, E). Figures are representative of three replicate experiments. Statistical significance was determined using Kruskal-Wallis with Dunn's correction (A) or Mann-Whitney test (D-H). *P < 0.05; **P < 0.01, ***P < 0.001; ****P < 0.0001; n.s. non-significant.

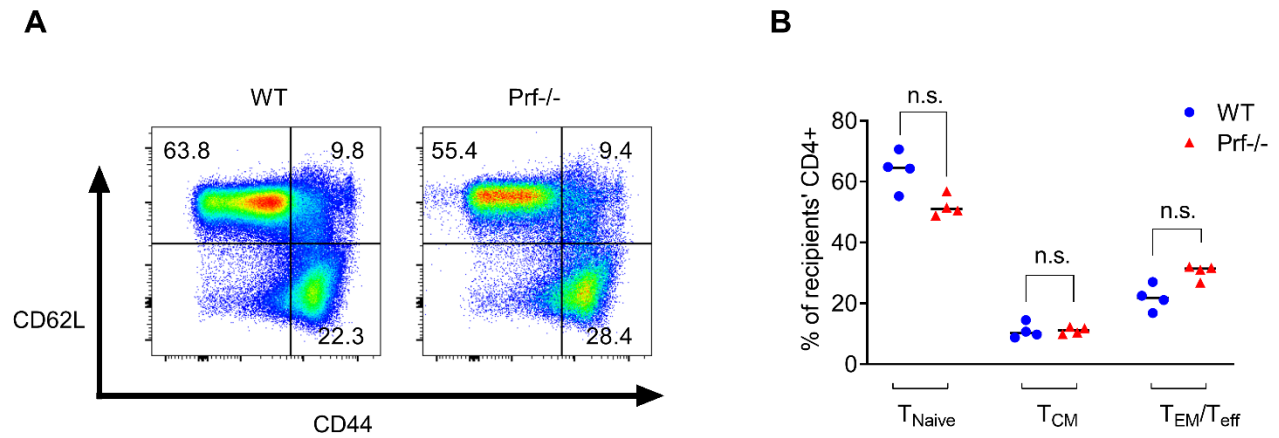


Figure S6. Phenotype of recipient-derived CD4⁺ T cells. Leukemia-bearing mice were treated with CAR-T (5E6 cells) according to the treatment scheme Figure 2A. (A) Representative dot plots and (B) statistical comparison of CD44-CD62L⁺ (T_{naive}), CD44⁺CD62L⁺ (T_{CM}), and CD44⁺CD62L⁻ (T_{EM} or T_{eff}) composition within recipient-derived CD4⁺ T cells (CD45.1⁺/CD45.2⁻/CD4⁺) are shown. Data are presented as means ± SD (B). n = 4 (B). Figures are representative of three replicate experiments. Statistical significance was determined using Kruskal-Wallis with Dunn's correction (B). *P < 0.05; **P < 0.01, ***P < 0.001; ****P < 0.0001; n.s. non-significant.

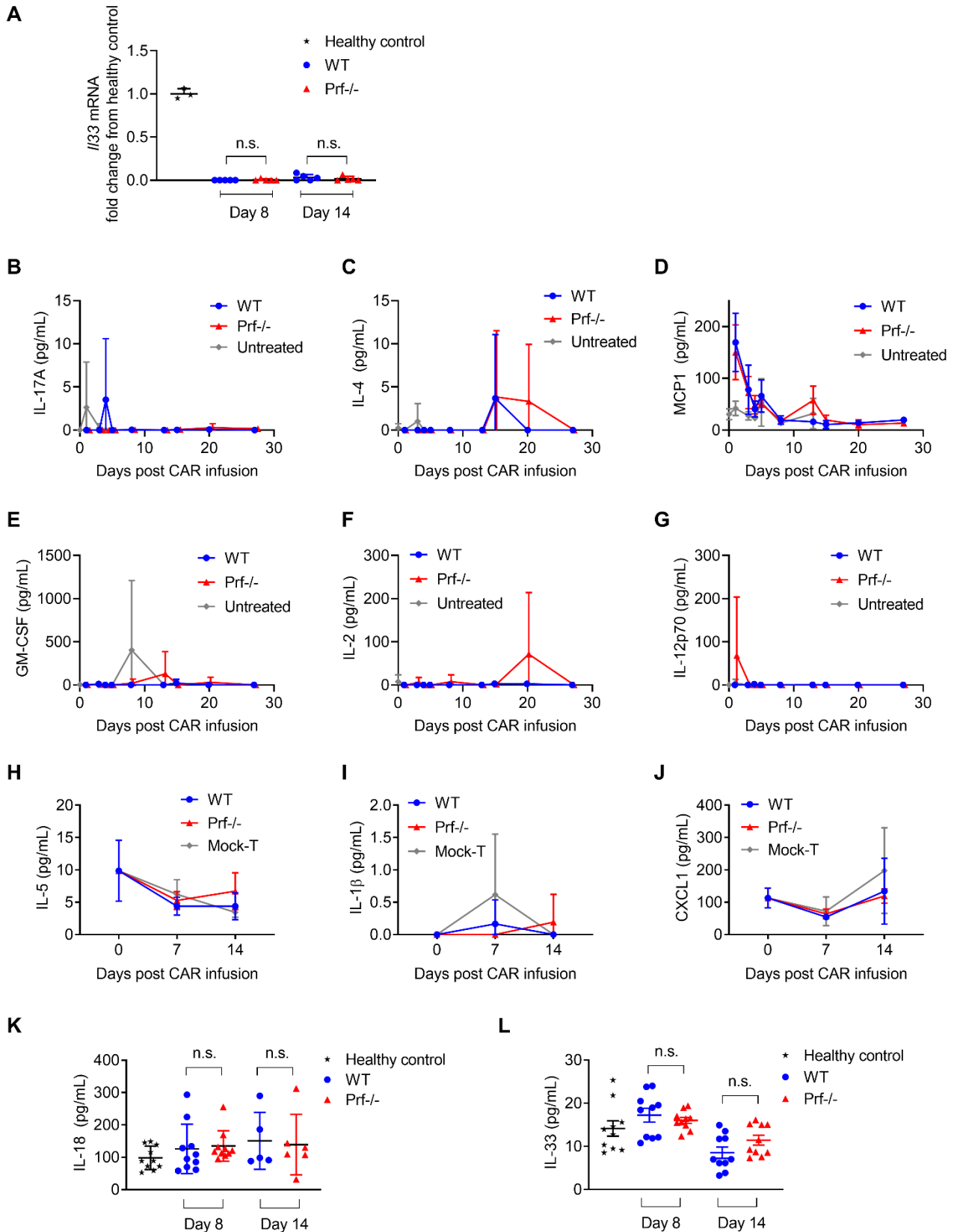


Figure S7. IL-33 transcripts and kinetics of serum cytokine levels in CAR-T recipients. Leukemia-bearing mice were treated with CAR-T (5E6 cells) according to the treatment scheme in Figure 2A. (A) Expression of IL-

33 gene in whole bone marrow on day 8 and day 14 were evaluated with RT-qPCR. Levels of (B) IL-17, (C) IL-4, (D) MCP1, (E) GM-CSF, (F) IL-2 and (G) IL-12p70 in CAR-T recipient serum were measured using Cytokine Bead Array on days 0, 1, 3, 4, 5, 8, 13, 15, 20, and 27 (n = 4). Levels of (H) IL-5, (I) IL-1 β , (J) CXCL1, and (L) IL-33 were measured by Meso Scale Discovery U-plex kit on days 0, 7 or 8, and 14 (n = 5 for H-J, n = 10 for L). (K) IL-18 was measured by ELISA on days 0, 8, and 14 (n = 10 on day 8, n = 6 on day 14). Healthy controls in A, K, and L represent data from age- and sex-matched untreated littermates. Data are presented as means \pm SD. Statistical significance was determined using Kruskal-Wallis with Dunn's correction (A, K, L). *P <0.05; **P <0.01, ***P <0.001; ****P <0.0001; n.s. non-significant.

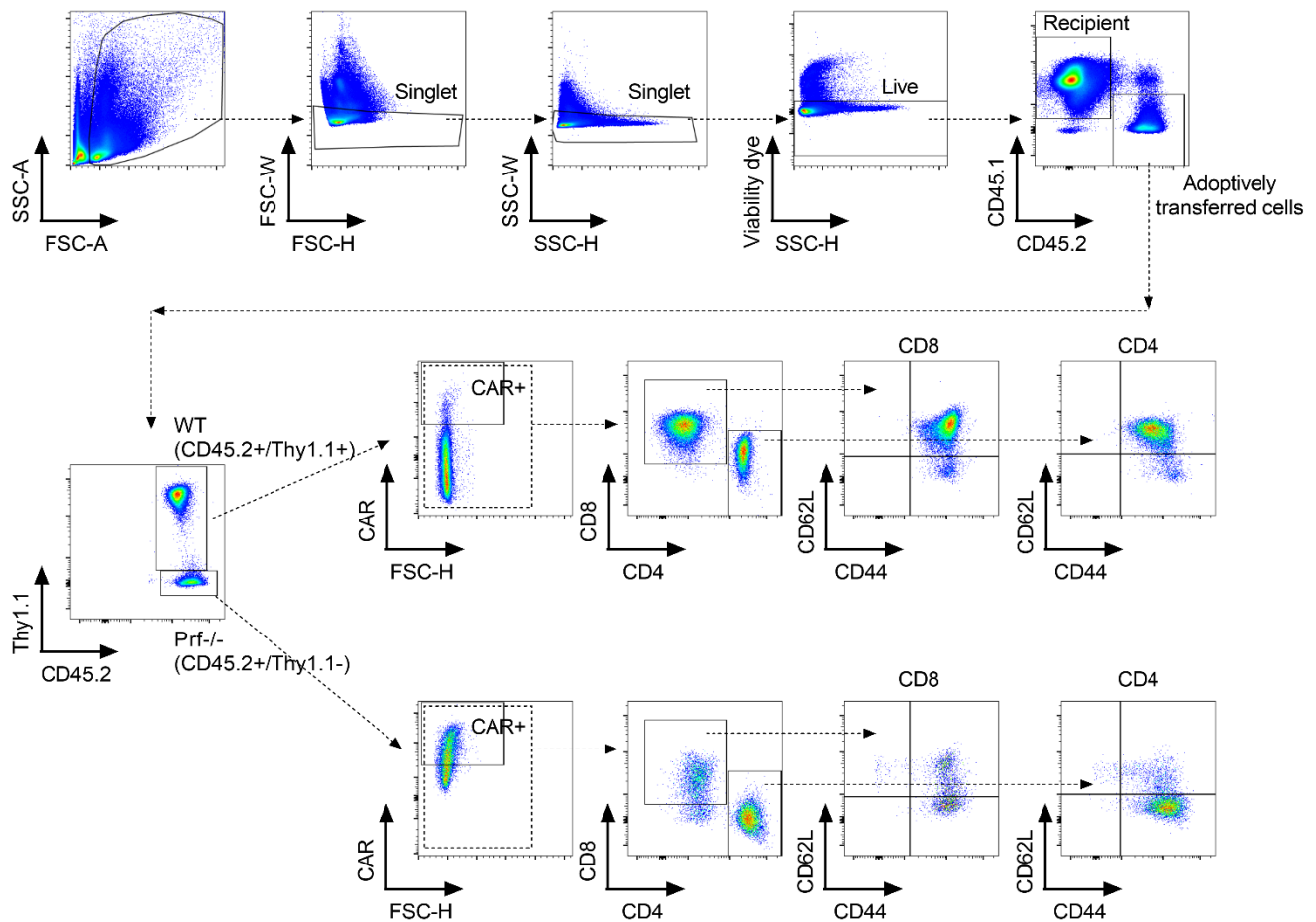


Figure S8. Gating strategy used for flow cytometry analyses of WT and Prf^{-/-} CAR-T following co-infusion into leukemia-bearing mice. Representative flow cytometry dot plots from one mouse co-injected with Prf^{-/-} CAR-T and WT untransduced T cells are shown to describe the gating strategy used for analyses. By day 7, recipient mice did not have detectable CD19⁺ cells, either leukemia or recipient-derived B cells, as depicted in Figure 3C-D.

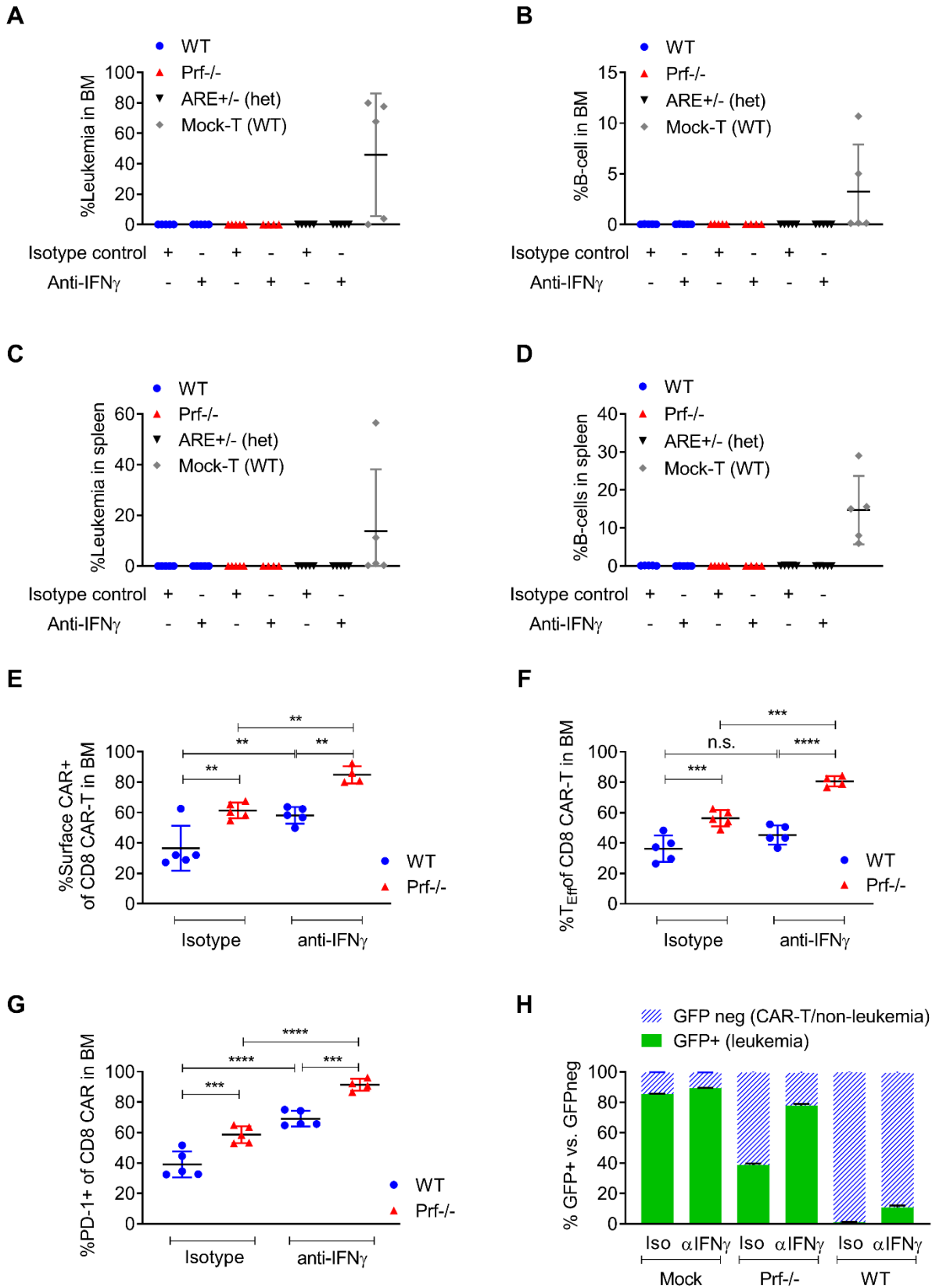


Figure S9. The effects of IFN γ neutralization on anti-leukemia cytotoxicity and phenotypes of CAR-T. (A-G) Leukemia-bearing mice were treated with CAR-T (5E6 cells), derived from either WT, Prf^{-/-}, or ARE-Del

(heterozygous) mice. Mice were treated with IFN γ neutralizing antibody or isotype control according to the treatment scheme Figure 7A. Leukemia (CD45.2+CD19+) and normal B-cell (CD45.2-CD19+B220+) in (A, B) bone marrow and (C, D) spleen were measured on day 13 of treatment, using flow cytometry analysis. On day 13 after adoptive T-cell transfer, (E) surface CAR expression, (F) the percentages of CD44+CD62L- (T_{EM} or T_{Eff}), and (G) PD-1 expression within the CD8+ CAR-T subset (CD45.2+CD8+) in recipients' bone marrow were assessed by flow cytometry. (H) WT CAR-T, Prf^{-/-} CAR-T, and WT untransduced T cells (Mock) were co-cultured with GFP-transduced CD19+ E2aPBX at an E:T ratio of 1:1 in the presence of either IFN γ neutralizing antibody (clone XMG1.2, BioXcell) or isotype control (rat IgG1 anti-horseradish peroxidase, BioXcell) 10 μ g/mL for 3 days. Then residual live E2aPBX (GFP+ fraction) within the co-culture was evaluated with flow cytometry. Data are presented as means \pm SD. n = 4-5 (A-G); n = 3 (H). Figures are representative of three replicate in vitro experiments and two representative in vivo experiments. Statistical significance was determined using one-way ANOVA with Sidak's correction (E-G). *P <0.05; **P <0.01, ***P <0.001; ****P <0.0001; n.s. non-significant.

Supplemental Table 1: Antibodies and reagents used for flow cytometry analysis

Target antigen	Clone	Conjugate	Company	Catalog #
CD3	145-2C11	PE-Cy7	BioLegend	100320
CD8a	53-6.7	FITC	eBioscience	11-0081-85
CD8a	53-6.7	APC-eFluor 780	eBioscience	47-0081-82
CD4	GK1.5	APC-Cy7	BioLegend	100414
CD4	GK1.5	BV711	BD Biosciences	563050
CD44	IM7	PerCP-Cy5.5	eBioscience	45-0441-82
CD44	IM7	PE-CF594	BD Biosciences	562464
CD62L	MEL-14	APC	eBioscience	17-0621-83
PD-1	J43	PE-Cy7	eBioscience	25-9985-82
PD-1	J43	BV650	BD Biosciences	744546
TIM3 (CD366)	8B.2C12	APC	eBioscience	17-5871-82
LAG3(CD223)	C9B7W	PerCP-Cy5.5	BioLegend	125212
CD45.1	A20	PE	eBioscience	12-0453-83
CD45.1	A20	FITC	eBioscience	11-0453-82
CD45.2	104	eFluor 450	eBioscience	48-0454-82
CD45.2	104	FITC	eBioscience	11-0454-85
CD45.2	104	PE-Cy7	BioLegend	109830
Thy1.1	HIS51	PE-Cy7	eBioscience	25-0900-82
CD19	eBio1D3	eFluor 450	eBioscience	48-0193-82
CD19	eBio1D3	PerCP-Cy5.5	eBioscience	45-0193-82
CD22	OX-97	APC	BioLegend	126110
B220	RA3-6B2	APC-Cy7	BioLegend	103224
CD107a	eBioH4A3	PE	eBioscience	12-1079-42
Mouse IgG1 kappa isotype control	P3.6.2.8.1	PE	eBioscience	12-4714-81
Protein L (Biotinylated)	N/A	N/A	Thermo Fisher Scientific	29997
Streptavidin	N/A	PE	eBioscience	12-4317-87
Viability dye (fixable)	N/A	eFluor 506	eBioscience	65-0866-14

Supplemental Table 2: Sequences of primers used for qPCR

Target gene	Forward primer (5' --> 3')	Reverse primer (5' --> 3')
pro-IL-1 β	TCTTTGAAGTTGACGGACCC	TGAGTGATACTGCCTGCCTG
IL-18	CAGGCCTGACATCTTCTG	CTGACATGGCAGCCATT
IL-33	ATTTCCCCGGCAAAGTTCAG	AACGGAGTCTCATGCAGTAGA
GAPDH	TGCACCACCAACTGCTTAG	GGATGCAGGGATGATGTTC

Supplemental Table 3: List of differentially expressed genes (greater than 2-fold changes) comparing Prf^{-/-} CD8⁺ CAR-T cells to WT CD8⁺ CAR-T cells after CAR-mediated in vitro activation

Gene ID	P-value	FDR step up	Fold change
Prf1	5.59E-10	3.68E-07	-7.27
Lmna	7.93E-13	4.18E-09	-4.13
Ms4a4c	5.34E-10	3.63E-07	-3.59
Efcab7	3.79E-10	2.95E-07	-3.54
Mptx2	6.34E-04	2.00E-02	-3.52
Efna3	3.23E-02	2.80E-01	-3.4
Gpr34	1.10E-09	6.28E-07	-2.93
Ehd3	8.11E-08	1.79E-05	-2.83
Samd3	1.35E-06	1.68E-04	-2.62
Sidt1	5.18E-09	2.23E-06	-2.55
Klrk1	7.84E-11	8.70E-08	-2.45
Tmem154	2.29E-05	1.57E-03	-2.39
Il18rap	8.39E-09	3.27E-06	-2.39
Dpy19l2	7.23E-03	1.09E-01	-2.37
Slc9a9	4.53E-09	2.03E-06	-2.37
Stpg4	6.21E-03	9.89E-02	-2.33
Trim65	3.11E-06	3.15E-04	-2.32
Tcf7	3.77E-06	3.71E-04	-2.32
Cd160	2.29E-08	7.36E-06	-2.3
Il18r1	1.73E-08	5.89E-06	-2.27
Plxnc1	3.46E-05	2.18E-03	-2.26
Ccr2	1.38E-09	7.25E-07	-2.26
Plin2	1.78E-06	2.06E-04	-2.25
Pla2g16	2.26E-06	2.46E-04	-2.2
Klrd1	4.02E-07	6.52E-05	-2.2
Capn12	1.77E-02	1.93E-01	-2.2
Misp	4.09E-02	3.21E-01	-2.16
Lax1	3.17E-07	5.39E-05	-2.16
D130020L05Rik	4.21E-03	7.60E-02	-2.15
Ipcef1	3.29E-08	9.61E-06	-2.14
Phf11b	1.48E-10	1.42E-07	-2.13
Prr19	2.14E-03	4.74E-02	-2.12
Nfe2l3	1.46E-03	3.68E-02	-2.08
Col27a1	9.51E-04	2.73E-02	-2.08
Ifi214	2.60E-06	2.74E-04	-2.07
Brms1	8.13E-04	2.42E-02	-2.05
Nnt	1.25E-06	1.59E-04	-2.05
Ifi213	2.04E-08	6.82E-06	-2.05
Skida1	2.14E-02	2.17E-01	-2.02
Cryge	3.45E-02	2.90E-01	-2.02

Cpt1a	5.19E-06	4.76E-04	-2.01
Vgll1	1.61E-02	1.83E-01	-2.01
Samsn1	2.18E-05	1.51E-03	2
Gbe1	1.81E-03	4.26E-02	2
Homer1	3.80E-05	2.34E-03	2.01
Alpl	1.06E-04	5.11E-03	2.01
H2-Ab1	2.72E-03	5.61E-02	2.01
Bnip3l	2.69E-06	2.81E-04	2.02
Pxdc1	1.32E-06	1.66E-04	2.03
Selenbp1	2.34E-03	5.02E-02	2.03
Auh	3.06E-07	5.29E-05	2.03
Zbtb38	1.20E-07	2.41E-05	2.04
Gsn	1.08E-02	1.41E-01	2.04
Crem	1.18E-06	1.53E-04	2.04
Fndc3a	1.68E-05	1.25E-03	2.05
Sccpdh	1.29E-04	6.06E-03	2.06
Tnfrsf18	1.35E-07	2.61E-05	2.06
Tcf4	1.24E-03	3.26E-02	2.06
Tmc6	2.05E-03	4.59E-02	2.06
Prdm1	5.05E-05	2.88E-03	2.07
Ndrp2	1.69E-05	1.26E-03	2.07
Dusp7	7.95E-04	2.37E-02	2.07
Ak4	9.36E-07	1.26E-04	2.09
Zeb2	1.53E-06	1.86E-04	2.1
Abhd18	2.14E-05	1.49E-03	2.11
Fam20c	1.71E-03	4.12E-02	2.12
Fosl2	2.07E-06	2.30E-04	2.13
Nsmf	2.61E-03	5.44E-02	2.13
Acs13	7.14E-04	2.18E-02	2.13
Blnk	2.40E-06	2.57E-04	2.14
Pmvk	1.52E-03	3.80E-02	2.14
Kdm6b	3.70E-07	6.08E-05	2.14
Dir2	5.05E-06	4.64E-04	2.15
Nfil3	1.59E-04	7.11E-03	2.15
Insig1	8.65E-07	1.18E-04	2.16
Rgs1	5.29E-06	4.81E-04	2.16
Ide	4.39E-07	6.95E-05	2.16
Aqp9	7.27E-10	4.50E-07	2.16
Vegfa	8.52E-04	2.51E-02	2.16
Msmo1	3.59E-08	9.94E-06	2.17
Tpd52	1.09E-07	2.25E-05	2.17
Tet2	7.06E-07	1.00E-04	2.17
Fam20a	3.05E-07	5.29E-05	2.17
Rnf19b	1.46E-06	1.80E-04	2.18

Gcnt2	4.34E-06	4.14E-04	2.18
Ncs1	3.82E-07	6.24E-05	2.19
Preli2	8.56E-07	1.18E-04	2.19
Tnfaip3	3.82E-05	2.35E-03	2.2
Serpinb1a	2.94E-05	1.90E-03	2.21
Irs2	1.53E-05	1.16E-03	2.21
Sdc4	5.24E-05	2.97E-03	2.22
Hmox1	2.31E-08	7.36E-06	2.23
Pnp2	1.90E-05	1.36E-03	2.25
Stxbp1	1.04E-07	2.17E-05	2.26
Batf2	1.34E-05	1.04E-03	2.27
Rnase12	1.68E-03	4.08E-02	2.27
Vmn1r4	5.24E-08	1.36E-05	2.28
Cysltr1	2.12E-06	2.34E-04	2.28
Pvr	1.43E-07	2.71E-05	2.28
Fcgr2b	1.30E-03	3.38E-02	2.28
Spp1	2.44E-06	2.59E-04	2.31
Tnfrsf4	2.00E-05	1.42E-03	2.31
Dntt	1.48E-04	6.68E-03	2.31
Txnrd3	3.08E-08	9.13E-06	2.32
Apbb2	4.25E-05	2.55E-03	2.33
Cited2	8.24E-08	1.79E-05	2.33
Socs3	1.42E-05	1.08E-03	2.33
Zfp36	1.68E-05	1.25E-03	2.34
Dusp3	1.10E-07	2.26E-05	2.34
Tspan9	7.86E-06	6.62E-04	2.34
Cdkn1a	2.69E-06	2.81E-04	2.35
H2-DMb1	1.21E-06	1.56E-04	2.38
Pth1r	2.73E-03	5.62E-02	2.38
Tec	7.53E-08	1.75E-05	2.38
Lyn	6.17E-08	1.51E-05	2.39
Ccng2	6.06E-06	5.34E-04	2.39
Cep170	4.42E-09	2.02E-06	2.42
Stk38l	4.46E-07	7.01E-05	2.44
Hilpda	7.64E-04	2.31E-02	2.44
Egln3	1.94E-06	2.20E-04	2.45
Il1a	8.13E-08	1.79E-05	2.47
Calcr1	3.02E-08	9.10E-06	2.47
Cxcl10	3.60E-05	2.24E-03	2.48
Cdh1	3.81E-04	1.39E-02	2.49
Frm4b	1.45E-09	7.46E-07	2.5
Ier3	5.06E-04	1.71E-02	2.51
Fads2	2.12E-03	4.73E-02	2.54
Adm	4.24E-04	1.51E-02	2.54

Csrnp1	5.96E-06	5.30E-04	2.54
P4ha2	2.22E-04	9.16E-03	2.55
Slc2a3	3.10E-07	5.32E-05	2.56
Rgcc	3.99E-06	3.87E-04	2.57
Scd3	2.27E-08	7.36E-06	2.58
Pde2a	1.42E-07	2.71E-05	2.59
Mzb1	1.74E-06	2.04E-04	2.59
Cd38	6.70E-06	5.83E-04	2.59
C1qtnf12	6.91E-07	9.90E-05	2.62
Cysltr2	3.79E-11	5.51E-08	2.62
Calhm6	2.31E-05	1.57E-03	2.69
Il9	1.35E-06	1.68E-04	2.7
Nr4a3	3.43E-07	5.69E-05	2.74
Pnp	1.82E-05	1.32E-03	2.74
Gem	1.48E-07	2.77E-05	2.77
Ero1l	1.17E-08	4.18E-06	2.78
Ube2l6	6.87E-06	5.89E-04	2.78
Ccl1	6.04E-07	8.93E-05	2.79
Cd24a	4.15E-03	7.52E-02	2.81
Metrn1	1.15E-07	2.34E-05	2.85
Nr4a2	5.63E-08	1.41E-05	2.85
A730081D07Rik	1.38E-05	1.05E-03	2.88
Ccl4	1.24E-05	9.64E-04	2.9
Cxcr4	9.82E-09	3.74E-06	2.9
Vpreb3	1.49E-06	1.81E-04	2.91
Iltifb	5.67E-04	1.85E-02	2.98
Ccl3	6.57E-06	5.74E-04	3.02
Ccl9	9.11E-08	1.96E-05	3.04
Iigp1	8.51E-07	1.18E-04	3.05
Tiparp	1.03E-06	1.36E-04	3.08
Cd79b	6.76E-07	9.75E-05	3.08
Swap70	1.30E-09	7.04E-07	3.08
Gm6455	1.69E-10	1.55E-07	3.09
Gm4841	2.52E-04	9.98E-03	3.09
Mycn	1.02E-07	2.14E-05	3.11
Cth	1.16E-10	1.22E-07	3.11
Plcx1	1.35E-04	6.27E-03	3.12
Cox6a2	3.45E-08	9.73E-06	3.14
Runx1	5.37E-09	2.26E-06	3.15
Gm21671	2.33E-05	1.58E-03	3.17
Atf3	6.82E-05	3.72E-03	3.21
Aldoc	4.92E-04	1.69E-02	3.25
St6gal1	1.79E-07	3.25E-05	3.26
Tnfrsf13c	2.11E-06	2.33E-04	3.27

Cd180	4.40E-05	2.58E-03	3.28
Il6	8.37E-06	6.97E-04	3.29
Lilr4b	7.50E-11	8.70E-08	3.29
Wdfy4	8.19E-08	1.79E-05	3.3
Lilrb4a	5.77E-11	7.15E-08	3.31
Bfsp2	4.69E-07	7.27E-05	3.31
Casp6	1.57E-11	3.01E-08	3.32
Dnajb4	2.07E-02	2.13E-01	3.36
Cnn3	6.30E-06	5.53E-04	3.38
Cdkn2a	1.32E-07	2.58E-05	3.4
Inhba	4.73E-09	2.08E-06	3.41
Il24	1.11E-13	1.17E-09	3.5
Plk2	1.40E-10	1.41E-07	3.51
Mxd1	5.43E-08	1.40E-05	3.58
Tmem176b	1.20E-09	6.64E-07	3.62
Etv5	8.03E-08	1.79E-05	3.63
Lrrc32	2.77E-06	2.88E-04	3.67
Gm17019	4.48E-08	1.18E-05	3.68
Themis2	4.14E-07	6.66E-05	3.73
Bank1	3.31E-09	1.60E-06	3.83
Cd19	1.29E-08	4.52E-06	4.09
Aldh2	4.91E-07	7.56E-05	4.18
Gm6460	6.83E-10	4.36E-07	4.37
Il22	3.19E-10	2.69E-07	4.39
Fzd7	8.23E-10	4.95E-07	4.4
Akt3	3.53E-10	2.86E-07	4.47
Ctla4	1.10E-09	6.28E-07	4.48
Cxcl9	1.76E-06	2.05E-04	4.53
Cybb	3.08E-10	2.69E-07	4.57
Gm5861	1.36E-08	4.71E-06	4.62
Il5	5.64E-06	5.05E-04	4.63
Speer6-ps1	1.56E-07	2.86E-05	4.64
Cd74	6.29E-05	3.48E-03	4.77
Ccr8	4.56E-10	3.31E-07	4.78
H2-DMb2	2.55E-07	4.56E-05	4.81
Pth	7.82E-08	1.79E-05	4.91
Ppp1r3b	6.27E-07	9.18E-05	4.97
Ndrp1	1.95E-06	2.20E-04	5.13
4933402N22Rik	5.29E-12	1.24E-08	5.15
Il10	6.20E-13	4.18E-09	6.11
Akr1c18	9.98E-13	4.21E-09	6.66
Gm14023	2.38E-14	5.02E-10	6.87
Cd81	7.43E-05	3.93E-03	7.17
Slc15a3	2.23E-11	3.92E-08	7.78

Pou2af1	4.02E-11	5.51E-08	8.29
Csf2	4.18E-11	5.51E-08	8.65
Ly86	1.93E-12	6.77E-09	9
Spi1	1.67E-09	8.39E-07	11.64
Bcl11a	2.66E-12	7.13E-09	13.84
Il13	2.71E-12	7.13E-09	14.36
Car2	2.44E-11	3.95E-08	15.12
Mef2c	4.21E-10	3.17E-07	16.86
Cd79a	7.64E-12	1.61E-08	27.66
Erdr1	3.46E-08	9.73E-06	80.84

Supplemental Text 1: Supplemental Methods

CD107a degranulation assay, cytotoxicity assay, and proliferation assay

For CD107a degranulation assay, 1E5 CAR-T and leukemia cells were co-incubated in 96-well round-bottom plates in complete mouse media (CMM) (the composition of CMM is detailed in the main text, method section). One hour after initiating the co-culture, 2 μ M monensin and 5 μ L of CD107a antibody or isotype control was added, and co-culture was continued for another 3 hours, and then stained for surface antibodies and analyzed by flow cytometry. For analysis of cytotoxicity, GFP-transduced E2aPBX (3E5 cells) were plated in 24-well poly-D-Lysine coated plates for 4 hours in 0.5mL CMM. CAR-T (6E5 cells) in 0.5mL CMM were then added to obtain an effector-to-target cell (E:T) ratio of 2:1. Killing was monitored in real-time with an IncuCyte Zoom (Essen BioScience); phase contrast and green fluorescent images were taken at indicated timepoints. Green objects (GFP+ leukemia) were counted at each timepoint and normalized to levels in wells with un-transduced T cells. Data were analyzed using IncuCyte Zoom Software ver. 2016B (Essen BioScience). For proliferation assay, CAR-T cells labeled with CellTrace Violet (Invitrogen, Thermo Fisher Scientific) were co-cultured with either CD19+ or CD19- E2aPBX at an E:T ratio of 1:1 for 3 days in 96-well plate, followed by flow cytometry analysis.

RT-qPCR of pro-IL-1 β , IL-18, and IL-33

RNA was purified using the RNeasy Plus Mini Kit (Qiagen), and cDNA was generated using Invitrogen SuperScript III Reverse Transcriptase (Invitrogen, Thermo Fisher Scientific) and ran on SimpliAmp Thermo Cycler (Thermo Fisher Scientific). Subsequently, qPCR was performed using Power SYBR Green PCR Master Mix (Applied Biosystems, Thermo Fisher Scientific) and StepOnePlus Real-Time PCR System (Thermo Fisher Scientific) according to the manufacturer's protocol. RNA levels were normalized to GAPDH. Primer sequences are listed in Supplemental Table 2.

Microarray and Nanostring: sample preparation and data acquisition

CAR-T cells were generated from CD3+ enriched WT or Prf^{-/-} mouse splenocytes (bulk CAR-T). After completion of transduction and the removal of Dynabeads Mouse T-Activator CD3/CD28 (Life Technologies), CAR-T were cultured for four days. Bulk CAR-T were then co-cultured with CD19+ E2aPBX at an E:T ratio of 1:1 (1E6 cells/mL). Following 24 hours of co-culture, CD8+ fraction of CAR-T were isolated using the CD8+ T Cell Isolation Kit (Miltenyi Biotec). As a pre-activation control, the

CD8⁺ fraction of CAR-T was isolated from the same bulk CAR-T used to set up co-culture, immediately prior to co-culture. Analyses were performed using 6 biological replicates for the activation group, and 3 biological replicates for the pre-activation group. Isolated CD8⁺ CAR-T were snap frozen on dry ice immediately following isolation, and RNA from all frozen samples was isolated in a single batch using the RNeasy Plus Mini Kit (Qiagen). Microarray processing was performed using the mouse Clariom S Array (Applied Biosystems) according to the manufacturer's protocol at the Frederick National Laboratory for Cancer Research (FNLCR). All statistical analyses of microarray data were performed with Partek Flow (Partek) genomic data analysis software using default parameters. Differentially expressed gene tables were generated and the presented analysis was performed using genes with $p < 0.05$ and a change in expression of >2-fold. Differentially expressed genes were analyzed using David version 6.8 (<https://david.ncifcrf.gov/home.jsp>) and functionally annotated using Go Gene Ontology Biologic Process (GOTERM_BP_Direct). All microarray data has been made publicly available at GEO accession number GSE130929.

For gene expression profiling of CAR-T recipient mice's bone marrow, recipients' bone marrows were harvested 14 days after CAR-T cell treatment, depleted of red blood cells using ACK Lysing Buffer (Lonza), and 1E6 cells were snap frozen on dry ice. RNA from all frozen samples were isolated in a single batch using the RNeasy Plus Mini Kit (Qiagen). Gene expression data were obtained in a single batch using Nanostring, nCounter Inflammation Panel Mouse v2 (NanoString Technologies) according to the manufacturer's protocol at the FNLCR. There were 5 biological replicates per group. Data were analyzed using nSolver Analysis Software version 4.0 for Windows (64-bit) and nCounter Advanced Analysis 2.0 (NanoString Technologies). Data were normalized based on the geometric means of the default positive controls and the panel of house-keeping genes as recommended by the manufacturer. QC and background thresholding were performed using the manufacturer's pre-set default parameters.

Supplemental Text 2: Modified definition of HLH/MAS-like toxicities used in our anti-CD22 CAR-T clinical trial

Peak ferritin level > 100,000 µg/L with at least two of the following criteria:

- Hepatic aminotransferase or bilirubin grade ≥ 3
- Creatinine grade ≥ 3
- Pulmonary edema grade ≥ 3
- Evidence of hemophagocytosis on bone marrow aspirate / biopsy

The criteria are modified version of the criteria used by Neelapu et al. in anti-CD19 CAR-T settings (Neelapu SS et al. *Nat Rev Clin Oncol*, 2018), which incorporates ferritin >10,000 µg/L as the cutoff. In our anti-CD22 CAR-T trial, median ferritin level was 65,288 µg/L, and the bottom 25 percentile level was 15,219 µg/L, and thus, the cutoff of >10,000 µg/L would have applied to the majority of patients regardless of presence or absence of other HLH-like clinical phenotypes. Therefore, in the current criteria, the value of ferritin >100,000 µg/L has been chosen as the cutoff (Shah NN et al. *J Clin Oncol*, 2020).

Supplemental Text 3: Primary HLH testing performed in anti-CD22 CAR-T trial

NK function or other primary HLH testing was infrequently performed (n = 3). In two cases, tests showed normal NK function and revealed no mutations pathognomonic of HLH. One patient, however, was found to have decreased NK cell function, suggesting that some patients may have a predisposition for HLH development. In this latter case, concurrent genetic testing was not performed.